Inorg. Chem. **2002**, *41*, 693–698

$AsCl_3$: From the Crystalline to the Liquid State. XRD (176 < *T* (K) < 250) and WAXS (295 K) Studies†

Jean Galy,*,‡ Renée Enjalbert,‡ Pierre Lecante,‡ and Andrzej Burian§

Centre d'Elaboration de Matériaux et d'Etudes Structurales (CEMES/CNRS), 29 Rue Jeanne Marvig, BP 4347, 31055 Toulouse Cedex 4, France, and Institute of Physics, University of Silesia, ul. Uniwersytecka 4, 40-007 Katowice, Poland

Received March 13, 2001

This paper presents structural studies on crystalline and liquid $AsCl_3$, performed using X-ray diffraction (XRD) and wide-angle X-ray scattering (WAXS) in the 176–250 K temperature range and at 295 K for the crystalline and liquid samples, respectively. The XRD results, collected using a single-crystal diffractometer, show that $AsCl_3$ crystallizes in the orthorhombic system with $P2_12_12_1$ space group and the unit cell parameters $a = 9.475(3)$ Å, $b = 11.331(2)$ Å, and $c = 4.2964(8)$ Å at 221 K. This structure is stable in the temperature range 176–243 K. Above the melting point, at 257 K, transition to the liquid state is observed. The WAXS data were recorded up to a maximum scattering vector $K_{max} = 16$ Å^{-1} and then converted to real space by the sine Fourier transform, yielding to the reduced radial distribution function (RRDF). For a series of models, based on the crystalline $AsCl_3$ structure, the intensity and RRDF functions have been computed and compared with the experimental data. These simulations indicate that the model consisting of six $AsCl_3$ molecules, arranged along the *y* axis, accounts satisfactorily for the experimental observation. The results of the structure analysis in both crystalline and liquid states are discussed in relation to the influence of the As lone electron pair.

Introduction

For a long time we have payed special attention to the compounds containing M* elements carrying a lone pair E because of their extremely rich chemistry and stereochemistry. In the former aspect they act very often as "structural scissors" with other chemical compounds based on normal or transition elements, building up mono- or two-dimensional networks, and in the latter aspect offer unusual one sided coordination. The lone pair E usually occupies the apex of a polyhedron formed by the firmly bounded anions: tetrahedron, square pyramid, trigonal bipyramid, or octahedron.

This original crystal chemistry was particularly emphasized by Andersson et al.[1] and Galy et al.[2] In the oxides and fluorides the volume of the sphere of influence of E was appreciated as the volume of an oxygen O^{2-} or a fluorine F^- anion, i.e., 16−18 Å.[3] On the basis of these principles the M*−E distances for Ge(II) to Br(V) ({Ar}$3d^{10}4s^2$), Sn(II) to Xe(VI) ({Kr}$4d^{10}5s^2$), and Tl(I) to Bi(III) ({Xe}$4f^{14}5d^{10}6s^2$) were derived.[2]

Later on an extensive study was carried out on the crystal chemistry of the VA element trihalides NX_3 to BiX_3 (X = F, Cl, Br, I).[3] All of these trihalides are characterized by a basic molecular unit M^*X_3. The steric effects of E have been appreciated on the basis of the centroïd of the electronic doublet designed by E_c which is closer to the nucleus than the center of the sphere of influence E_s. The correlative variations of M*−E_c and M*−E_s have been studied according to the nature of M*.

In the present paper our aim is to appreciate if molecular association via weak interactions existing in the solid state remain in the liquid state. For such purpose, we followed the crystalline-state evolution of $AsCl_3$ between 176 and 250 K and after melting ($T_f = 257$ K) to the liquid state, using successively X-ray single-crystal diffraction (XRD) and wide-angle X-ray scattering (WAXS).

Experimental Section

$AsCl_3$ Crystal Structure. The crystal structure of $AsCl_3$ (253 K) was determined for the first time together with that of PCl_3

* To whom correspondence should be addressed. Phone: 33 5 62 25 78 11. Fax: 33 5 62 25 79 99. E-mail: galy@cemes.fr.
† Dedicated in memory of Olivier Kahn (1942−1999).
‡ CEMES/CNRS.
§ University of Silesia.

(1) Andersson, S.; Åström A.; Galy, J.; Meunier, G. *J. Solid State Chem.* **1973**, *6*, 187.
(2) Galy, J.; Meunier, G.; Andersson, S.; Åström, A. *J. Solid State Chem.* **1975**, *13*, 142.
(3) Galy, J.; Enjalbert, R. *J. Solid State Chem.* **1982**, *44*, 1.

10.1021/ic0102788 CCC: $22.00
Published on Web 01/23/2002

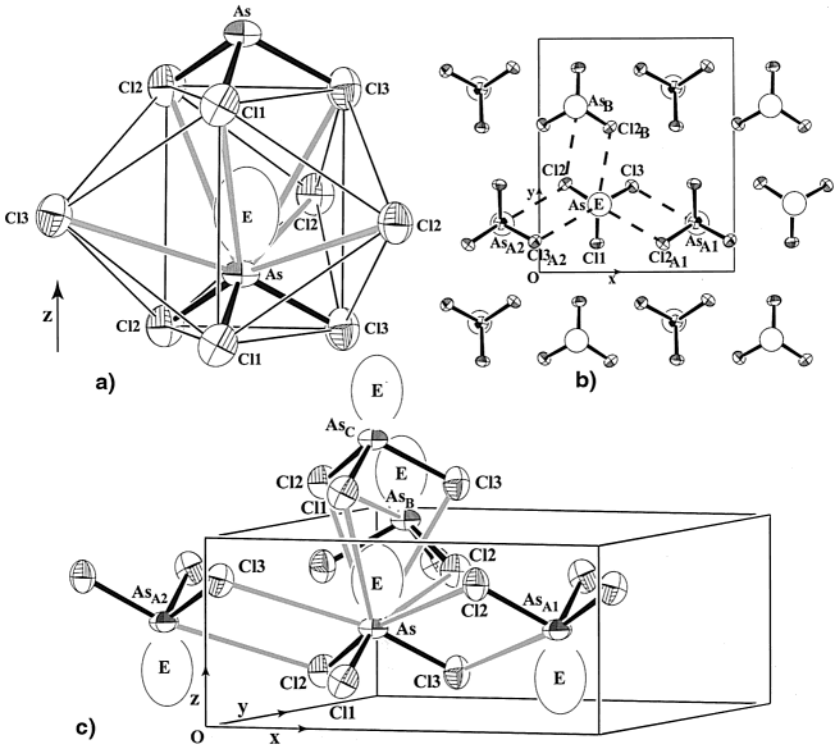

Figure 1. (a) $AsCl_3$ molecule; (b) projection of the structure onto the (001) plane; (c) closest environment of one $AsCl_3$ molecule. The ellipsoïds are drawn at 75% probability.

Table 1. Crystallographic Data for $AsCl_3$ at $T = 221$ K

empirical formula	$AsCl_3$	fw	181.27
a (Å)	9.475(3)	space group	$P2_12_12_1$ (No. 19)
b (Å)	11.331(2)	T (°C)	−52
c (Å)	4.2964(8)	λ(Mo Kα) (Å)	0.710 73
V (Å^3)	461.3(4)	ρ_{calc} (g cm^{-3})	2.61
Z	4	μ(Mo Kα) (cm^{-1})	88.9
R1(F_o)[a]	0.038	wR2(F_o)[b]	0.093

[a] $R1 = [\Sigma|F_o| - |F_c|]/[\Sigma|F_c|]$. [b] $wR2 = \{[\Sigma w(F_o^2 - F_c^2)^2]/[\Sigma w(F_o^2)^2]\}^{1/2}$.

(133 K) and PBr_3 (193 K) after in situ crystal growth at low temperature directly onto an automatic CAD4-Nonius X-ray diffractometer.[4,5] $AsCl_3$ crystallizes in the orthorhombic system, space group $P2_12_12_1$, with the parameters $a = 9.475(3)$ Å, $b = 11.331(2)$ Å, and $c = 4.2964(8)$ Å at $T = 221$ K. The data concerning the X-ray investigation are listed in Table 1. The structural determination has been conducted to a low R factor, $R = 0.038$. Important interatomic distances and angles are listed in Table 2.

In this structure the $AsCl_3$ molecules are stacked in the [001] direction making an infinite "triangular tube" of chlorine atoms. The arsenic atoms with their lone pair E are located in chlorine triangular prisms formed by the three directly covalently bounded chlorines and the ones of the following molecule along [001]. Arsenic atom establishes As−Cl interactions with three adjacent molecules, the chlorines forming a tricapped triangular prism around AsE. According to the Galy and Enjalbert[3] proposal concerning stereochemical influence of the lone pair E, appreciated in terms of the sphere of influence and clearly seen in this $AsCl_9$ tricapped triangular prism, it is possible to localize its center at the barycenter of the nine chlorines. The coordinates of E are $x = 0.3106$, $y = 0.2906$, and $z = 0.7432$; the As−E distance is then 1.10 Å, in agreement with numerous analogous distances calculated in various structures.[2] A perspective view of this crystalline architecture and a projection along [001] are depicted in Figure 1a,b.

Table 2. Main Intra- and Interatomic Distances (Å) and Angles (deg) of $AsCl_3$ Molecule in Its Tricapped Triangular Prism at Various Temperatures

	176 K	221 K	235 K	243 K
As−Cl1 (Å)	2.164(3)	2.158(2)	2.162(4)	2.162(3)
As−Cl2 (Å)	2.173(3)	2.163(3)	2.176(4)	2.163(4)
As−Cl3 (Å)	2.164(3)	2.163(3)	2.162(4)	2.165(4)
Cl1−As−Cl2 (deg)	98.3(1)	98.4(1)	98.5(1)	98.5(1)
Cl2−As−Cl3 (deg)	97.3(1)	97.5(1)	97.3(1)	97.2(1)
Cl3−As−Cl1 (deg)	97.8(1)	97.8(1)	97.8(1)	97.6(2)
Cl1−Cl2 (Å)	3.281(5)	3.271(3)	3.285(4)	3.276(4)
Cl2−Cl3 (Å)	3.259(4)	3.252(3)	3.256(4)	3.246(4)
Cl3−Cl1 (Å)	3.263(4)	3.255(3)	3.257(5)	3.255(4)
As−$Cl1_C$ (Å)	3.667(4)	3.701(2)	3.714(4)	3.706(4)
As−$Cl2_C$ (Å)	3.702(4)	3.742(2)	3.747(4)	3.745(4)
As−$Cl3_C$ (Å)	3.755(2)	3.782(2)	3.801(4)	3.790(4)
$AsCl2_{A1}$ (Å)	3.842(4)	3.865(3)	3.887(4)	3.881(4)
As−$Cl2_B$ (Å)	3.952(4)	3.975(2)	3.978(6)	3.978(5)
As−$Cl3_{A2}$ (Å)	3.673(5)	3.711(3)	3.722(5)	3.722(4)

Experimental XRD at 176 < *T* (*K*) < 250. A droplet of $AsCl_3$ was inserted in a Lindemann capillary under dry argon atmosphere. The sealing was performed in order to create a small Lindeman glass bubble, the size of which ($\phi = 0.3$ mm; $L = 5$ mm) is smaller than the diameter of the cold nitrogen stream for the sake of temperature homogeneity of $AsCl_3$ after crystallization, and to prevent "caloduc" effects. The liquid was then frozen by the cold nitrogen stream; using a tungsten wire heater, a small zone was melted and the wire slowly moved along the bubble allowing the germination and crystallization of $AsCl_3$ (Figure 2).[3,5]

Finally the obtained single crystal was a cylinder of ∼0.7 mm long (Figure 3).

After the crystal quality was checked (Figure 4), a series of full crystal structure determinations were performed at various temperatures: 176, 184, 191, 198, 203, 206, 213, 221, 228, 235, 243, and 250 K.

(4) Enjalbert, R.; Galy, J. *C. R. Acad. Sci.* **1978**, *C287*, 259.
(5) Enjalbert, R. Thèse d'Université, No. 352, Toulouse, France, 1980.

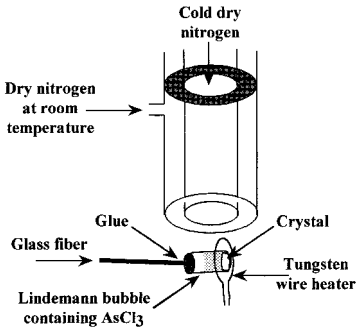

Figure 2. Schematic drawing of the crystal growth device.

Wide-Angle X-ray Scattering Study 295 K. The wide-angle X-ray scattering (WAXS) technique is quite suitable for the study of middle range order in amorphous solids and liquids. To do so, we have developed a special software the "Liquid and Amorphous Structure Investigation Package" (LASIP)[6] and built up an automatic diffractometer especially devoted to particular collection of suitable WAXS data. This conventional $\omega-2\theta$ diffractometer is equipped with a molybdenum target tube ($\lambda = 0.710\ 69$ Å), a flat graphite monochromator mounted in the incident beam, and a scintillation detector. Lindeman glass capillary ($\phi = 0.3$ mm and $L = 20$ mm) with $AsCl_3$ was placed on the goniometer axis. The data were recorded in the scattering vector range between 0.3 and 16 $Å^{-1}$ at 295 K.

The scattering vector is defined as $K = 4\pi \sin\theta/\lambda$, where 2θ is the scattering angle and λ is the wavelength. The stability of the X-ray flux and of the sample was checked from the reproducibility of successive scans. An additional measurement was made for the empty capillary in order to subtract the intensity scattered by the capillary from the total recorded intensity. The data were then corrected for fluorescence, absorption, polarization, and the Compton scattering.[7] The tabulated Compton intensities given by Hajdu[8] were taken for this correction. The fluorescence correction method, developed for a symmetrical transmission geometry, was adopted for the case of a cylindrical sample, according to our earlier paper.[9] Finally, the data were normalized to electron units using the high-angle method and converted to real space by the sine Fourier transform yielding to the reduced radial distribution function (RRDF).

Another experiment performed at 353 K (closer to the boiling point, 303 K) does not reveal any significant change in the scattered intensity.

Results and Discussion

$AsCl_3$ in the Solid State. The evolution of the cell parameters versus the various temperatures is depicted in Figure 5. It can be seen that after an almost linear increasing from 176 K up to ~221 K, the three parameters smoothly tend asymptotically toward limits indicating that the crystal architecture is close to vanishing around 250 K (the solid $AsCl_3$ melts at 257 K). In this temperature range, i.e., 176−250 K, the $a-c$ parameters exhibit significant discrepancies in their relative expansions: +1% for *a*, +0.6% for *b*, and 1.4% for *c*. As examples the main crystallographic data for only four structure determinations are reported in Table 2.

It is readily seen that the main structural features of the $AsCl_3$ molecule itself do not evolve with temperature; i.e., As−Cl bonds, Cl−As−Cl angles, and Cl−Cl distances remain practically unchanged in agreement with previous study.[4] The crystalline characteristics of $AsCl_3$ molecules are almost identical to those in the gas phase, the corresponding values, established by the gas electron diffraction[10] technique, being As−Cl = 2.162(3) Å, Cl−As−Cl = 98.6(6)°, and Cl−Cl = 3.278(4) Å. More important to understanding the mechanism of the solid ⇒ liquid transformation is, of course, to take into account the weak interactions between the As atom of one molecule toward the chlorines of neighboring ones. In that respect it is interesting to note that the distances increase significantly:

with ⟨As···Cl⟩ varying from 3.667 up to 3.706 Å and from 3.952 to 3.978 Å

and ⟨Cl···Cl⟩ varying from 3.608 up to 4.110 Å.

Inspecting Figure 1c, which is relative to the determination at 221K, we note that the reference molecule exhibits three types of intermolecular As−Cl interactions:

with the molecules denoted A1 and A2, related by the 2_1 axis along *a* (Figure 1; $\pm a/2$ translation), they exchange four interactions $As\cdots Cl2_{A1} = As_{A2}\cdots Cl2 = 3.863(3)$ Å and $As\cdots Cl3_{A2} = As_{A1}\cdots Cl3 = 3.711(3)$ Å;

with the molecule B, related by the 2_1 axis along *b* (Figure 1), two interactions $As\cdots Cl2_B = As_B\cdots Cl2 = 3.975(2)$ Å;

and with the molecule C, related by direct translation *c*, three interactions $As\cdots Cl1_C = 3.701(2)$ Å, $As\cdots Cl2_C = 3.742(2)$ Å, and $As\cdots Cl3_C = 3.782(2)$ Å, the lone pair E being inserted between these interaction lines. The distance increase with temperature due to these interactions is more significant in the [001] direction.

$AsCl_3$ in the Liquid State. For disordered materials the diffraction pattern arises from the coherent interference of scattered waves from distributed atoms as scattering centers. In the case of liquid, the averaged overall orientation intensity per average atom can be written as

$$I(K) = \frac{1}{N}\sum_{i=1}^{N}\sum_{j=1}^{N} f_i(K)\, f_j(K)\frac{\sin(Kr_{ij})}{Kr_{ij}} \exp\left(-\frac{1}{2}\sigma_{ij}K^2\right) \quad (1)$$

where N denotes the number of atoms, $f_i(K)$ is the atomic scattering factor of the ith atom, r_{ij} indicates the distance between the ith and jth atoms, and σ_{ij} is the standard deviation of r_{ij}.

The scattering data can be converted to real space by the inverse Fourier transform yielding the RRDF:

$$d(r) = 4\pi r[\rho(r) - \rho_0] = \frac{2}{\pi}\int_0^{K_{max}} \frac{Ki(K)}{\langle f\rangle^2} W(K)\sin(Kr)\, dK \quad (2)$$

where ρ_0 is the number density, $W(K)$ is the window function, $i(K) = I(K) - \langle f^2\rangle$ is the reduced intensity,

(6) Lecante, P.; Mosset, A.; Galy, J. *J. Appl. Crystallogr.* **1985**, *18*, 214.
(7) *International Tables for Crystallography*; The International Union of Crystallography, Kluwer Academic Publishers: Dordrecht, The Netherlands, 1992; Vol. C, pp 219−222.
(8) Hajdu, F. *Acta Crystallogr. A* **1972**, *28*, 250.
(9) Lecante, P.; Mosset, A.; Galy, J.; Burian, A. *J. Mater. Sci.* **1992**, *27*, 3286.
(10) Konaka S.; Kimura M. *Bull. Chem. Soc. Jpn.* **1970**, *43*, 1693−1703.

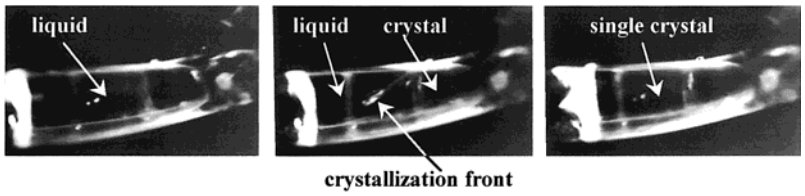

Figure 3. Germination of $AsCl_3$ single crystal in the Lindeman capillary.

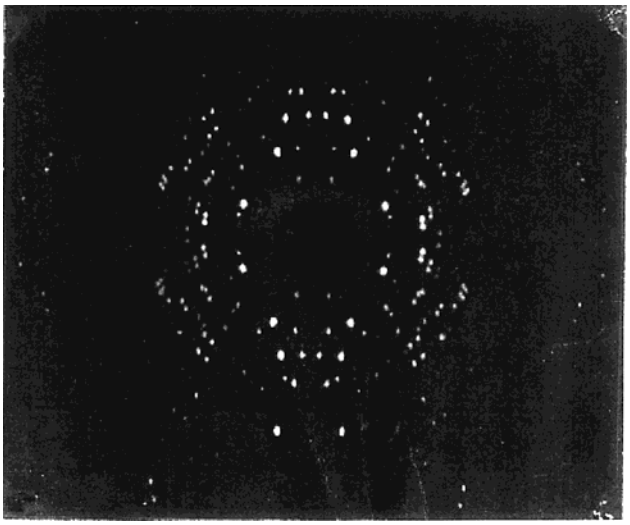

Figure 4. X-ray diffraction pattern of the $AsCl_3$ single crystal.

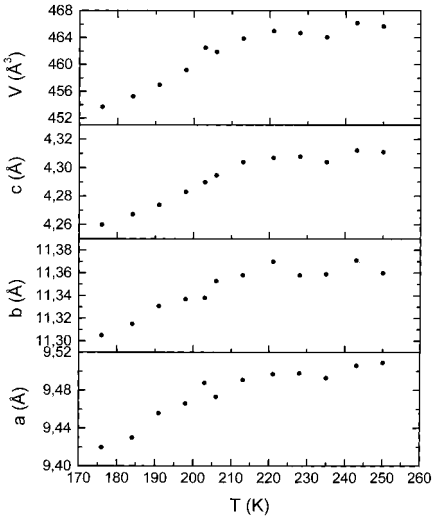

Figure 5. Evolution of crystal cell parameters (Å) versus temperature (K).

$$\langle f^2\rangle = \frac{1}{N}\sum_{i=1}^{N} f_i^2(K), \quad \langle f\rangle = \frac{1}{N}\sum_{i=1}^{N} f(K)$$

In the present work the Lorch window function $W(K) = [\sin(\pi K/K_{max})]/[(\pi K/K_{max})]$ was used for computation of the RRDF. The values of the atomic scattering factors were taken from the tables given by Waasmaier and Kirfel.[11] The radial distribution function $4\pi r\rho(r)$ provides information about the probability of finding an atom in a spherical shell at a distance r from an arbitrary atom. Successive peaks correspond to nearest-, second-, and next-neighbor atomic distribution.

(11) Waasmaier, D.; Kirfel, A. *Acta Crystallogr. A* **1995**, *51*, 416.

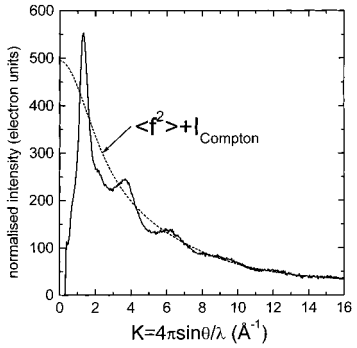

Figure 6. Normalized intensity function $I(K)$ and independent term $\langle f^2\rangle + I_{Compton}$.

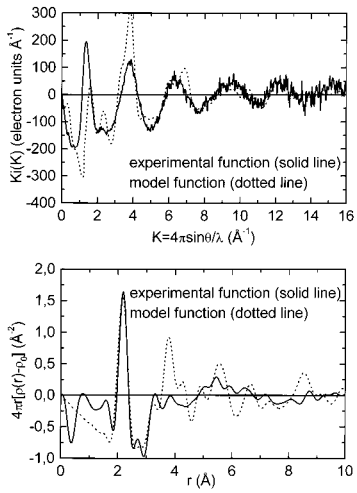

Figure 7. $Ki(K)$ (eu $Å^{-1}$) and RRDF ($Å^{-2}$) drawn according to the crystalline $AsCl_3$ structure, together with the experimental data.

The normalized intensity function *I(K)* is shown in Figure 6 together with the independent term $\langle f^2\rangle + I_{Compton}$. The intensity curve oscillates around the independent intensity, which indicates that the correction and normalization procedures were satisfactorily performed. Attempts have been made to simulate the experimental intensity and reduced radial distribution functions via eqs 1 and 2 using models based on the crystalline $AsCl_3$ structure.

Liquid−Solid Structural Relations. We have considered a series of models in which the local atomic arrangement of the $AsCl_3$ crystal is preserved in the liquid state. The basic building blocks are $AsCl_3$ triangular prisms arranged along three axes *x*, *y*, and *z*. To compare efficiently experimental functions with the simulated ones based on hypothetical models dealing with the possible medium range order of $AsCl_3$ molecules, the curves $Ki(K)$ and RRDF are drawn in Figures 7−11.

The RRDF shown here were obtained from measures performed at 295 K. The RRDF (in atomic units) expressed

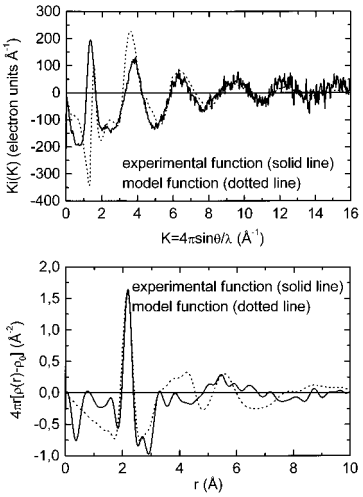

Figure 8. *Ki*(*K*) (eu Å^{-1}) and RRDF (Å^{-2}) drawn according to the molecular pilling along the [001] direction in the crystal−$(AsCl_3)_C$ molecules, together with the experimental data.

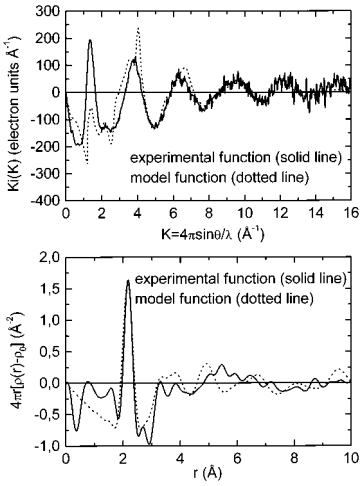

Figure 9. *Ki*(*K*) (eu Å^{-1}) and RRDF (Å^{-2}) drawn according to the molecular pilling along the [100] direction in the crystal−$(AsCl_3)_{A1}$ and $(AsCl_3)_{A2}$ molecules, together with the experimental data.

versus interatomic distances (in angstroms) shows defined peaks which positions are directly correlated to As−As, As−Cl, or Cl−Cl distances and which amplitudes depend on the scattering factors of the envisaged atomic pairs. Obviously some organization at the middle distance remains in the liquid, as indicated by defined peaks existing up to 7−8 Å, i.e., above the most important intramolecular distance Cl−Cl of 3.29 Å, showing that there is some repeatable associations of a few molecules.

Taking into account that an average regular $AsCl_3$ molecule defined from the crystal structure at 235 K shows ⟨As−Cl⟩ = 2.161 Å, ⟨Cl−Cl⟩ = 3.266 Å, and ⟨Cl−As−Cl⟩ = 97.9° and that in the gas phase, as found by the gas electron diffraction technique, such values are As−Cl = 2.162(3) Å, Cl−As−Cl = 98.6(6)°, and Cl−Cl = 3.278(4) Å.

It can be concluded that the molecule in the liquid state is very similar to the one in the solid and gas phases. Such an assertion is fully confirmed by the positions of the first two peaks of the RRDF (Figures 7−9) which maxima are estimated to be 2.178 and 3.30 Å. The first one corresponds

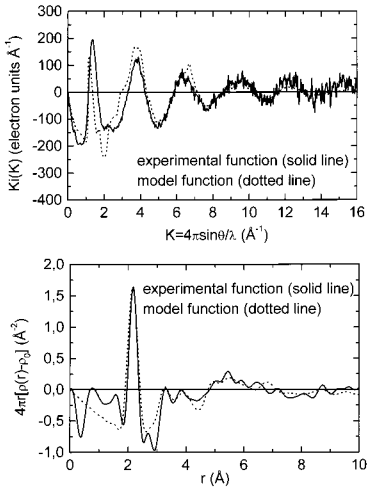

Figure 10. *Ki*(*K*) (eu Å^{-1}) and RRDF (Å^{-2}) drawn according to the molecular pilling along the [010] direction in the crystal−$(AsCl_3)_B$ molecules, together with the experimental data.

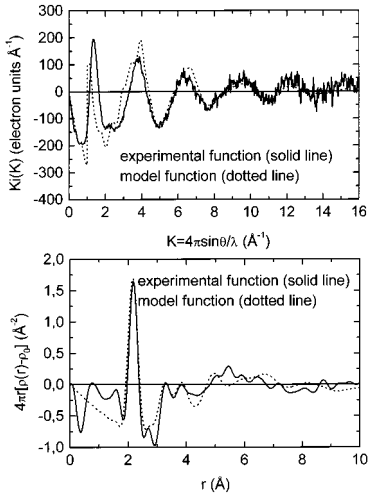

Figure 11. *Ki*(*K*) (eu Å^{-1}) and RRDF (Å^{-2}) drawn according to the double bridge dimers and opposite lone pairs with $(AsCl_3)_A$, $(AsCl_3)_B$, and $(AsCl_3)_{A1}$ molecules, together with the experimental data.

to As−Cl bonds and compares well with preceding values (only +0.02 Å). The same occurs for the intramolecular Cl−Cl interatomic distances, which are 3.28 Å. Such values imply a bond angle ⟨Cl−As−Cl⟩ = 98.1° which is right between the observed ones in the solid and gas states. First attempts have been made to simulate the reduced intensity and radial distribution functions respectively by the model consisting of 36 atoms placed inside the 10 Å × 10 Å × 10 Å box and arranged according to the crystalline $AsCl_3$ structure. The results of this simulation are compared with the experimental data in Figure 7. The structural parameters are listed in Table 3. It is clear that the crystalline model, based on the $P2_12_12_1$ symmetry, does not account for the experimental data. The simulated RRDF exhibits many more structural features than the experimental function, and no simple transformation of the crystalline structure could improve the agreement with the experimental data. In the next step fragments of the crystalline state were considered as the basis of the liquid model. However, the first coordination RRDF peak was precisely reproduced by intramolecular ordering, in which each As is bonded to three Cl.

Table 3. Structural Parameters for the Model Based Calculations of the *Ki*(*K*) and *D*(*r*) Functions, Shown in Figures 7−11

crystalline model 36 atoms inside 10 Å × 10 Å × 10 Å box		6 $AsCl_3$ molecules arranged along the [001] direction		6 $AsCl_3$ molecules arranged along the [100] direction		6 $AsCl_3$ molecules arranged along the [010] direction		6 $AsCl_3$ molecules with doubly bridged dimers		expt
r (Å)	*σ* (Å)	*r* (Å)	*σ* (Å)	*r* (Å)	*σ* (Å)	*r* (Å)	*σ* (Å)	*r* (Å)	*σ* (Å)	*r* (Å)
2.16−10.0	0.07	2.16	0.07	2.16	0.08	2.16	0.08	2.16	0.08	2.18
		3.26	0.15	3.26	0.15	3.26	0.07	3.25−4.10	0.12	3.30
		3.70−4	0.20	3.71−10.0	0.25	3.64−6.13	0.10	4.80−6.00	0.20	3.85
		5.35−10.0	0.30			6.49−10.0	0.20	6.05−10.0	0.30	

Coming back to the crystal structure and taking into account the shortest As−Cl intermolecular distances (⟨3.75 Å⟩) between the reference molecule $AsCl_3$ and the one repeated by the *c* translation, i.e., $(AsCl_3)_C$, the first hypothesis assuming the partial destruction of the three-dimensional order was to postulate for a breaking of the weak As−Cl interaction existing between the $(AsCl_3)_n$ stacks. The clearly seen minimum in the RRDF at 4.3 Å ($c = 4.2964$ Å) destroys completely such hypothesis and emphasizes the repelling role of the lone pair E toward the molecule $(AsCl_3)_C$. These shortest $\langle As-Cl\rangle_C$ intermolecular distances are by no means real arsenic−chlorine interactions, the lone pair E exhibiting a real screening effect well directed along the pseudo-3-fold axis of the molecule. It can be concluded that the $AsCl_3$ molecules are stacked in the *c* direction via the three-dimensional organization of the molecules. As soon as the crystal melts, the repulsion between E and the chlorine base of the following $AsCl_3$ molecule along the [001] direction becomes preponderant and the piling disappears. Both RRDF and *Ki*(*K*) simulations, implying molecules along *c*, illustrate clearly this fact, with a maximum on the RRDF model function opposite to the experimental minimum and a poor agreement on the second one (Figure 8).

A second hypothesis which was evaluated was a possible association between the molecules lying in the [100] direction. Possible interactions are $(AsCl_2)_{A1}$ and $(AsCl_3)_{A2}$ (see Table 2). These molecules constitute dipoles alternatively disposed. The lone pair E of As atoms does not disrupt too much such interactions established (as seen in Figure 1) below its sphere of influence. The tentative model gives RRDF and *Ki*(*K*) simulations, shown in Figure 9, which do not reproduce satisfactorily the experimental data, especially with the important peak at 5 Å and the deep well at 5.5 Å, where a maximum is clearly appearing in the experimental curve. Moreover the first diffraction peak, appearing at about $K = 1.3$ Å^{-1}, is not reproduced by the model.

Finally, better agreement was found with the model implying six molecules exhibiting ordering at a middle range in the [010] direction. The rather well-defined peaks at 3.29, 3.83, 5, and 5.5 Å are reasonably fitted, and the *Ki*(*K*) function also shows good agreement between experimental and calculated curves (Figure 10). This fact indicates that some "memory" of the molecules distribution has been saved after the crystal melting. We note that such interactions, which occur in the [010] direction, correspond to the lowest expansion among cell parameters (i.e. *b*) when the crystal is progressively heated from the lowest temperatures to the melting point. A tentative understanding of such reminiscent association could be linked with the fact that the lone pair E of the basic molecule As "sees" directly As_B ($E-As_{A1} = 5.00$ Å) while the other cations As_{A1} and As_{A2}, despite similar distances ($E-As_{A1} = 4.84$ Å; $E-As_{A2} = 5.01$ Å), are screened by chlorine atoms.

We also tested out the model with doubly bridged dimers and opposite lone pairs and As···Cl about 3.80 Å. Such an arrangement was constructed with six molecules $AsCl_3$ molecules, implying As in the A, B, and A1 positions. The comparison of the model based simulation and the experimental data is shown in Figure 11. The model parameters are listed in Table 3. Agreement between the simulation and the experiment is good up to about 4 Å, but in the region of 5−6 Å a clear misfit is observed. This model does not account better for the experimental data than that with the $AsCl_3$ molecules arranged along the [010] direction.

To conclude, it is demonstrated in this paper the persistence of some molecular association in liquid $AsCl_3$, similar to those encountered in the built up three-dimensional network of the solid phase. Another interesting point suggested by this paper is that the interaction between the lone pair of one molecule with the cation of a neighbor one occurs, but additional studies on similar systems seem to be necessary. Worthy of note is that the main features of the isolated molecule $AsCl_3$, As−Cl bond lengths, Cl−Cl interatomic distances, and Cl−As−Cl angles, are extremely close in the three crystal, liquid, and gas states.

Acknowledgment. A. Burian wishes to thank the Centre National de la Recherche Scientifique for a special grant, during which strong collaboration has been reinforced between our laboratories.

Supporting Information Available: X-ray crystallographic file in CIF format. This material is available free of charge via the Internet at http://pubs.acs.org.

IC0102788